Variation in Bufadienolide Composition of Parotoid Gland Secretion From Three Taxa of Japanese Toads

Takato Inoue[1] · Ryu Nakata[1,2] · Alan H. Savitzky[3] · Naoko Yoshinaga[1] · Akira Mori[4] · Naoki Mori[1]

Abstract

Toads of the genus *Bufo* synthesize and accumulate bufadienolides (BDs) in their parotoid glands. BDs are cardiotonic steroids that play an important role in defense against the toads' predators. Three bufonid taxa occur in mainland Japan, *Bufo japonicus formosus*, *B. j. japonicus*, and *B. torrenticola*. The chemical structures of BDs isolated from *B. j. formosus* were studied several decades ago, but there is no further information on the toxic components of Japanese toads and their metabolism. In this study, we analyzed BDs of toads from throughout Japan and compared the BD profiles by liquid chromatography/mass spectrometry (LC/MS) and hierarchical cluster analysis (HCA). We observed BDs in three taxa of Japanese toads, and identified five of the most common BDs by nuclear magnetic resonance (NMR) analyses. Of the five BDs, only bufalin was detected in all individuals. HCA of individual BD profiles divided the three taxa into five primary clusters and several subclusters. This result indicates that BD profiles differ both among and within the taxa. The clustering pattern of BDs is generally concordant with a phylogenetic tree reconstructed from the mitochondrial cytochrome *b* gene of Japanese toads. Our results suggest that the BDs of Japanese toads have diversified not in response to specific selective pressures, but simply due to population structuring over evolutionary time.

Introduction

Many vertebrates sequester toxins for defense, including poison frogs, some natricine snakes, and *Pitohui* birds. Those species acquire toxins from their prey and accumulate them in the skin, internal organs, feathers and muscles (Dumbacher


✉ Naoki Mori
mori.naoki.8a@kyoto-u.ac.jp

[1] Division of Applied Life Science, Graduate School of Agriculture, Kyoto University, Kitashirakawa, Sakyo, Kyoto, Kyoto 606-8502, Japan

[2] Present address: Department of Bioscience and Biotechnology, Kyoto University of Advanced Science, 1-1 Nanjo Otani, Sogabe, Kameoka, Kyoto 621-8555, Japan

[3] Department of Biology, Utah State University, Logan, UT 84322-5305, USA

[4] Department of Zoology, Graduate School of Science, Kyoto University, Kitashirakwa, Sakyo, Kyoto 606-8502, Japan

et al. 2004; Mori et al. 2012; Takada et al. 2005). On the other hand, toads (Bufonidae) synthesize and store toxins known as bufadienolides (BDs) in concentrated granular glands, and especially in the large, paired parotoid glands (Hostetler and Cannon 1974; Porto et al. 1972;). When harassed, viscous white fluid containing BDs is secreted from these glands (Fig. 1a) (Barbosa et al. 2009; Hutchinson and Savitzky 2004; Lichtstein et al. 1992). BDs function by inhibiting the activity of Na$^+$/K$^+$ ATPase, similar to other cardiotonic steroids (Yang et al. 2015). Due to this toxicity, there are few natural enemies of toads (Licht and Low 1968; Mohammadi et al. 2018; Shimada et al. 1977; Toledo and Jared 1995;).

Two species of toads, *Bufo japonicus* and *B. torrenticola*, are distributed in mainland Japan, and *B. japonicus* includes two recognized subspecies, *B. j. japonicus* and *B. j. formosus*. The distribution and morphology of Japanese toads, and feeding ecology of some populations of *B. j. formosus* have been well documented (Hirai and Matsui 2002; Matsui 1984), but knowledge about their BDs is limited. The chemical structures of BDs in *B. j. formosus* were studied several decades ago (Shimada et al. 1974; Shimada et al. 1976; Shimada et al. 1977), but the presence and identity of BDs in *B. j. japonicus* and *B. torrenticola* have not been studied. Moreover, toxin

Fig. 1 Toads and collection sites. (a) Parotoid gland of *B. japonicus formosus*; arrow indicates parotoid gland with white secretion being released. (b) Left, *B. j. japonicus*: middle, *B. torrenticola*; right, *B. j. formosus*. (c) The collecting localities of all sampled toads from seven districts of mainland Japan: Tohoku, Kanto, and Chubu districts (eastern Japan) and Kansai, Chugoku, Shikoku, and Kyushu districts (western Japan)
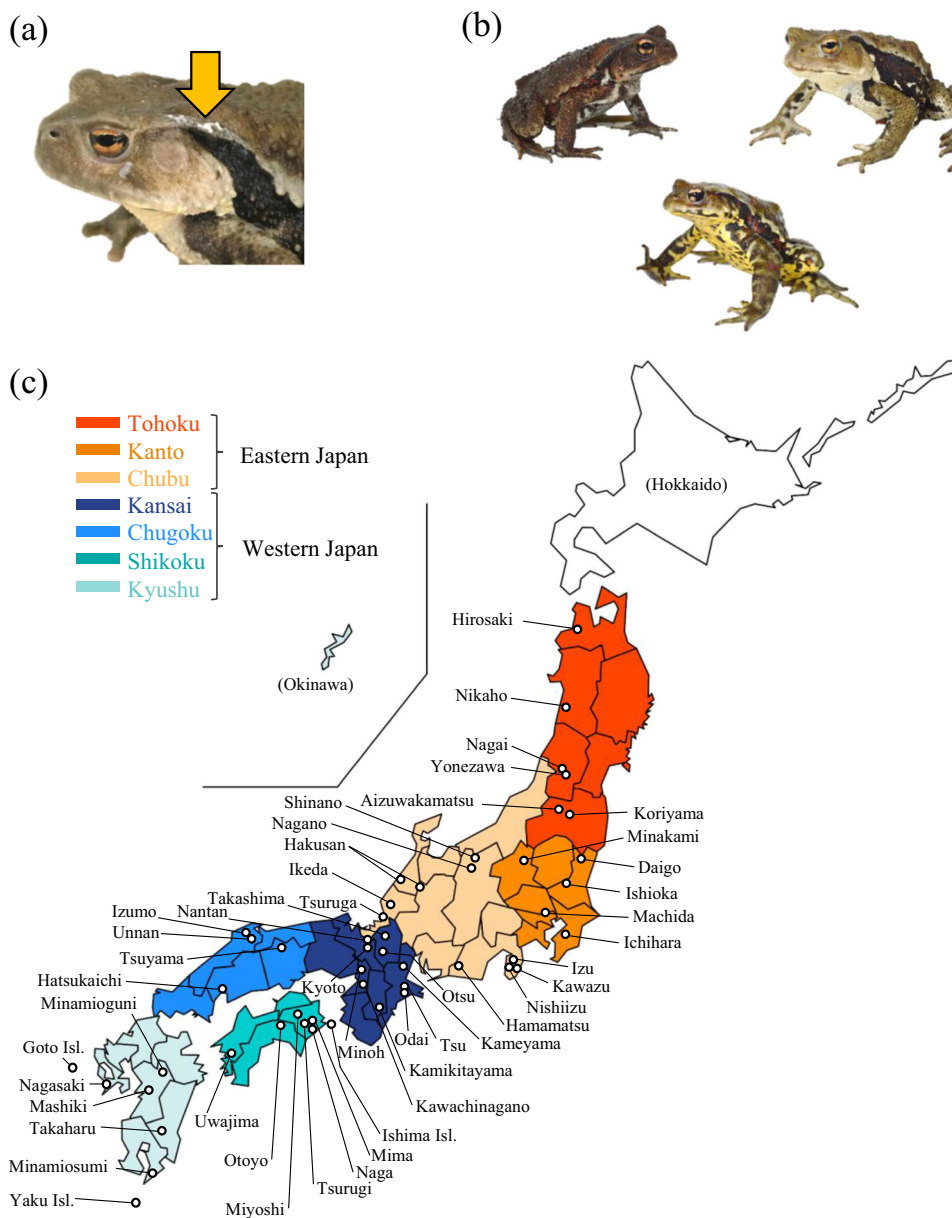
profiles of individual toads have not been compared, even among specimens of *B. j. formosus*. The defensive toxins of some animals diversify in response to selective pressure from predators or vary geographically (Brodie III and Brodie Jr 1999; Hanifin 2010; König et al. 2015; Roelants et al. 2010; Williams et al. 2003; Yoshida et al. 2020), but diversity of defensive toxins in most animal taxa has been poorly understood (Casewell et al. 2013; Mebs 2001). Thus, an analysis of the BD profiles of individual *B. japonicus formosus*, *B. j. japonicus*, and *B. torrenticola* from various localities in Japan would help in understanding the evolutionary history of Japanese toads and the metabolic system underlying the synthesis of BDs.

In this study, LC/MS and NMR were used to analyze the BDs in the parotoid secretion of toads collected from various

areas of mainland Japan. Hierarchical cluster analysis (HCA) of BD profiles revealed diversity both within and between the three Japanese bufonid taxa. Our data document both similarities and differences in BD profiles among Japanese toads and provide insights into their ecological and evolutionary significance.

Materials and Methods

Study Species and their Ranges Two species in the genus *Bufo*, one of which has two subspecies, occur in mainland Japan (Matsui and Maeda 2018) (Fig. 1c and Supplemental Table S1). *Bufo japonicus formosus* is distributed in eastern Japan (Tohoku, Kanto, and Chubu districts) and part of the

Kansai district. *Bufo j. japonicus* is distributed in western Japan (Kyushu, Shikoku, and Chugoku districts) and part of the Kansai district. *Bufo torrenticola* is distributed in part of the Kansai and Chubu districts. The two species were identified based on differences in the size of the tympanum (Matsui 1984).

Extraction of BDs from Toads Parotoid gland secretion was obtained by squeezing both glands with Kimwipes (Wiper S-200; Nippon Paper Crecia Co., Ltd., Tokyo, Japan) while wearing nitrile or latex gloves. Each Kimwipe was immersed in about 3 ml of MeOH within a glass vial with a Teflon-lined cap and stored at −20 °C in the dark. The immersed Kimwipe was washed with 5 ml of MeOH; then, both the MeOH storage and rinse solutions were combined and concentrated to dryness under reduced pressure. The crude extract (ext.) was weighed, dissolved in MeOH at a concentration of 1–10 mg ext./ml, and filtered with a syringe filter (DISMIC-13HP, pore diameter, 0.45 μm; Roshi Kaisha Ltd., Tokyo, Japan). This filtrate was mixed with digitoxigenin (as an internal standard, IS) and diluted to the concentration of 200 ng ext./μl and 25 ng/μl of IS.

LC/MS and LC/MS/MS Analyses LC/MS was carried out with a Prominence HPLC system coupled with LCMS-2010 (Shimadzu Co., Kyoto, Japan). A reversed-phase column (Mightysil RP-18 GP 50 × 2.0 mm I.D., 5 μm particle size; Kanto Chemical Co., Inc., Tokyo, Japan) was eluted (0.2 ml/min) with a gradient of 20% (0–2 min), 20–55% (2–20 min), 55–100% (20–35 min), and 100% (5 min) MeOH in H_2O containing 0.1% formic acid. The column temperature was maintained at 40 °C. The MS was operated in APCI positive ion mode with nebulizer gas flow of 2.5 l/min, APCI voltage of 1.9 kV, temperature of 400 °C, CDL temperature of 250 °C, and heat block temperature of 200 °C. The scan range for m/z values was 350 to 1000. LC/MS/MS was performed on an Ultimate 3000 SD UHPLC system coupled with LTQ Orbitrap discovery (Thermo Fisher Scientific Inc., MA, United States). A Unison UK-C18 column (75 × 2.0 mm I.D., 3 μm particle size; Imtakt Co., Kyoto, Japan) was eluted (0.2 ml/min) with a gradient of 0% (0–2 min), 0–25% (2–15 min), 25–99.5% (15–27 min), and 99.5% (27–37 min) acetonitrile in H_2O (both solvents containing 0.1 % formic acid). The column temperature was maintained at 50 °C. The MS was operated in ESI positive ion mode with the following parameters: capillary temperature of 380 °C, sheath gas flow rate of 5 (arb. unit), aux gas flow rate of 6 (arb. unit), sweep gas flow rate of 0 (arb. unit), source voltage of 4.5 kV, source current of 100 μA, capillary voltage of 33 V, tube lens voltage of 80 V. MS full scan was acquired in 30,000 resolution at m/z 100–1500. Automatic gain control (AGC) was set at $5 × 10^5$ with one micro scan and 500-msec maximum ion injection time. The MS/MS scan was operated by data

dependent acquisition (DDA) in 30,000 resolution at m/z 100–1500. AGC was set at $2 × 10^4$ with one micro scan and 1000-msec maximum ion injection time. For dynamic exclusion, repeat count was set at 1; repeat duration and exclusion duration were set at 30 and 20 s, respectively. The most intense ion was selected for collision induced dissociation (CID) with the following parameters: default charge state, 1; isolation width of m/z 2.0; normalized collision energy, 35; acquisition Q, 0.250; acquisition time, 30 msec; minimum signal required, 1000. The exact mass of diisooctyl phthalate ([M + H]$^+$ = 391.28429) was used for the lock mass.

BDs were characterized using UV absorption spectroscopy, which showed a maximum absorbance at 290–300 nm by the common moiety of a pyrone ring (Green et al. 1985). Each BD was tentatively named as a combination of a number and a letter; the number is the m/z value of the predicted [M + H]$^+$ ion, and the letter, in alphabetical order, was assigned to represent the elution order of BDs possessing the same numerical value.

Isolation of 8 BDs for Structural Analysis The crude extracts from 2 adult *B. j. formosus* and 24 adult *B. j. japonicus* were mixed and concentrated to dryness under reduced pressure to yield 104 mg extract (E1). Similarly, 233 mg extract (E2) was obtained from 29 adult *B. j. formosus* and 5 adult *B. j. japonicus*. E1 was fractionated with a Sep-Pak Vac (5 g) C18 Cartridge (Waters Co., Milford, MA), using a stepwise gradient of MeOH/H_2O mixtures (30/70, 50/50, 60/40, 70/30, 100/0; v/v, 2 × 40 ml each, except for 30/70 and 100/0 (1 × 80 ml each)) to give fraction i (46 mg), ii-1 (7 mg), ii-2 (12 mg), iii-1 (34 mg), iii-2 (56 mg), iv-1 (9.5 mg), iv-2 (trace) and v (trace), in eluted order. E2 was fractionated with a Sep-Pak Vac (5 g) C18 Cartridge (Waters Co., Milford, MA), using a stepwise gradient of MeOH/H_2O mixtures (30/70, 40/60, 50/50, 60/40, 70/30, 100/0; v/v, 2 × 40 mL each, except for 30/70, 70/30, and 100/0 (1 × 80 ml each)) to give fraction I (79 mg), II-1 (7.6 mg), II-2 (2 mg), III-1 (6.2 mg), III-2 (13.5 mg), IV-1 (30.3 mg), IV-2 (15.7 mg), V (trace) and VI (trace), in eluted order. Only gamabufotalin had been isolated in fraction II-1. Further fractionation was conducted using a Prominence HPLC system equipped with a UV-Vis detector (Shimadzu Co., Kyoto, Japan). A reversed-phase column (Mightysil RP-18 GP 250 × 4.6 mm I.D., 5 μm particle size; Kanto Chemical Co., Inc., Tokyo, Japan) was maintained at 40 °C and eluted under isocratic conditions at 1.0 ml/min flow rate. MeOH and H_2O (0.1% formic acid) were used for elution, mixed at an optimized ratio. Detection was carried out at 300 nm. Bufotalin (t_R, 8.3–9.1 min) was isolated from fraction iii-1 with 60% MeOH elution. Bufotalin-3-suberoyl-arginine ester (t_R, 4.4–5.6 min) was isolated from fraction iv-1 with 65% MeOH elution. Arenobufagin (t_R, 20.0–21.7 min) was isolated from fraction III-1 with 40% MeOH elution. 6α-Hydroxybufalin (t_R, 14.3–16.5 min) was isolated from

fraction III-2 with 50% MeOH elution. Bufalin (t_R, 11.9–13.2 min) was isolated from fraction IV-1 with 60% MeOH elution. Resibufogenin (t_R, 44.1–46.4 min) and cinobufagin (t_R, 46.8–50.0 min) were isolated from fraction IV-2 with 50% MeOH elution. The separation scheme is summarized in Supplemental Fig. S1.

NMR Spectroscopic Analyses NMR spectra were measured with a Bruker AV-400 III Spectrometer (400 MHz; Bruker BioSpin K.K., Kanagawa, Japan). BDs were dissolved in CD_3OD (>99.8% D, <0.03% H_2O; Euriso-Top, Saint-Aubin, France) containing 0.1% TMS or in $CDCl_3$ (99.8% D; Euriso-Top, Saint-Aubin, France) containing 1% TMS as an internal standard (δ_H, 0 ppm; δ_C, 49.15 ppm (CD_3OD) or 77.43 ppm ($CDCl_3$)). ^1H, ^{13}C, H-HCOSY, HSQC, HMBC and NOESY spectra were acquired. Data for ^1H-NMR were reported as follows: chemical shift (δ, ppm), multiplicity (s, singlet; d, doublet; t, triplet; q, quartet; sext, sextet; m, multiplet; br, broad), integration, and coupling constant (Hz).

Identification of Suberoyl Moiety of Bufotalin-3-Suberoyl-Arginine Ester (B3sa) The presence of suberic acid in B3sa was revealed by GC/MS analysis after hydrolysis and methyl esterification of the carboxylic acid according to the previous method in Zhao et al. (2010) and Hashimoto et al. (1981) with slight modifications. Two hundred μg of B3sa isolate was dissolved in 100 μl of 10% HCl aq./dioxane mixture (v/v = 1/1) and heated in a heat block at 80 °C for 3 h. The reactant was neutralized with 130 μl of 1.2 M $NaHCO_3$ aq. and washed with 100 μl of ethyl acetate three times. The aqueous layer was acidified with 2 ml of 1 M HCl aq. and separated with 5 ml of ethyl acetate three times. Ethyl acetate layers were combined and concentrated to dryness under reduced pressure. This concentrate was dissolved in 12 μl of toluene/MeOH mixture (v/v = 4/1) and mixed with 6 μl of trimethylsilyl-diazomethane (ca. 0.60 M in hexane; Tokyo Chemical Industry Co., Ltd., Tokyo, Japan). Thirty min later the aliquot of reactant was analyzed by GC/MS after the addition of the internal standard, naphthalene (12.5 ng/μl; FUJIFILM Wako Pure Chemical Co., Osaka, Japan). GC/MS analysis was performed using a gas chromatograph (HP-5890 series 2 Plus; Hewlett-Packard Co., Palo Alto, CA, United States) connected to a quadrupole mass spectrometer (HP-5989B; Hewlett-Packard Co., Palo Alto, CA, United States) in electron ionization (EI) mode (75 eV) and splitless mode. GC separation was performed on a capillary column (HP-5MS, 30 m × 0.25 mm I.D., 0.25 μm thickness; Hewlett-Packard Co., Palo Alto, CA, United States), with helium as the carrier gas (1.0 ml/min). The inlet and detector temperatures were 240 °C and 290 °C. The column oven was kept at 100 °C for 2 min from the start, then heated to 320 °C at 15 °C/min and kept at 320 °C for 6 min. The scan range for m/z values was 33 to 550. Authenticated standards of adipic acid

(>99.0%, Tokyo Chemical Industry Co., Ltd., Tokyo, Japan), pimeric acid (>99.0%, FUJIFILM Wako Pure Chemical Co., Osaka, Japan), and suberic acid (>98.0%, FUJIFILM Wako Pure Chemical Co., Osaka, Japan) were derivatized and analyzed by the same procedure. The concentration of standards in the injection sample was 12.5 ng (dicarboxylic acid equivalent)/μl.

Statistical Analyses RStudio ver. 1.1.463 (RStudio, Boston, MA, United States) and Excel 2016 (Microsoft, Redmond, WA, United States) were used for statistical analyses and data plots. The BD composition of each individual, obtained by the LC/MS analyses, was represented by a nominal scale (i.e., absence, 0; presence, 1) for 132 variables representing all of the compounds detected in any individual in this study (Supplemental Table S1). The dissimilarity between individuals was defined as simple matching distance (SMD): 1 minus the simple matching coefficient (SMC), SMD = 1−SMC and HCA was carried out by the Ward method (using R for Windows 3.5.2 package, "cluster ver. 2.1.0"). We performed an analog of the "elbow method," calculating the sum of squared errors of prediction (SSE), to assess the proper number of major clusters. Here, we assumed that the large change of SSE from k = 1 to 2 is natural, and looked for elbow points after k = 3, as in previous studies (Syakur et al. 2018; Kodinariya and Makwana 2013; Marutho et al. 2018).

Results

Inter- and Intra-Taxon Variation in BD Profiles LC/MS analyses confirm that *B. j. japonicus* and *B. torrenticola* accumulate BDs, as does *B. j. formosus* (Fig. 2). A total of 132 peaks were characterized as BDs (Supplemental Table S1). Among them, five BDs showed a high degree of commonality among the three taxa, and 36 BDs were unique to a single taxon (Table 1). The five common BDs were identified as gamabufotalin, arenobufagin, 6α-hydroxybufalin, bufalin, and resibufogenin (Fig. 3a). (Full details are described in the section *Structure of BDs*, below.)

In order to evaluate the differences among the BD profiles within and among the three taxa, we performed HCA and determined the proper number of clusters using the elbow method. The resulting dendrogram is shown in Fig. 4. The elbow curve plot identifies five major clusters. There is a strong change in the curve between k = 2–4 and k = 6–8, identifying k = 5 as the elbow point. Following this result, clusters C1–5 were recognized at the level shown by the broken line in Fig. 4, as follows: C1, mainly *B. j. formosus* in eastern Japan (Tohoku, Kanto, and Chubu districts); C2, *B. torrenticola* in part of Kansai district (Odai and Kamikitayama); C3, mainly *B. j. formosus* in Kansai district; C4, mainly *B. j. japonicus* in Kyushu district; C5, mainly *B. j. japonicus* in Kansai,

Table 1 Detection rates of 8 BDs identified in the present study and 36 BDs unique to each taxon

BD name	B. j. japonicus (N=46) (%)	B. j. formosus (N=70) (%)	B. torrenticola (N=16) (%)
Gamabufotalin	67	88	73
Arenobufagin	100	100	93
6α-Hydroxybufalin	100	100	94
Bufalin	100	100	100
Resibufogenin	100	100	71
Cinobufagin	28	100	99
Bufotalin	50	100	96
B3sa	37	0	10
397a	30	0	0
401e	20	0	0
399b	11	0	0
431b	7	0	0
415d	4	0	0
741a	4	0	0
457a	0	51	0
713a	0	16	0
461a	0	10	0
769a	0	9	0
671b	0	7	0
755b	0	7	0
743a	0	6	0
729g	0	4	0
757a	0	4	0
741b	0	4	0
485a	0	3	0
699c	0	3	0
713c	0	3	0
771c	0	3	0
461b	0	0	25
443c	0	0	19
475b	0	0	19
657b	0	0	19
729c	0	0	19
431a	0	0	13
459b	0	0	13
699b	0	0	13
727b	0	0	13
401j	0	0	6
685a	0	0	6
715a	0	0	6
729e	0	0	6
743b	0	0	6
771a	0	0	6
785a	0	0	6

Chugoku, and Shikoku districts. Each of the three taxa was present in several different clusters on the basis of its BD profiles and, except for C2, every cluster included individuals from more than one taxon. Therefore, we conclude that the BD profiles differ both among and within the three taxa. We also note that there is a general distinction between the BD
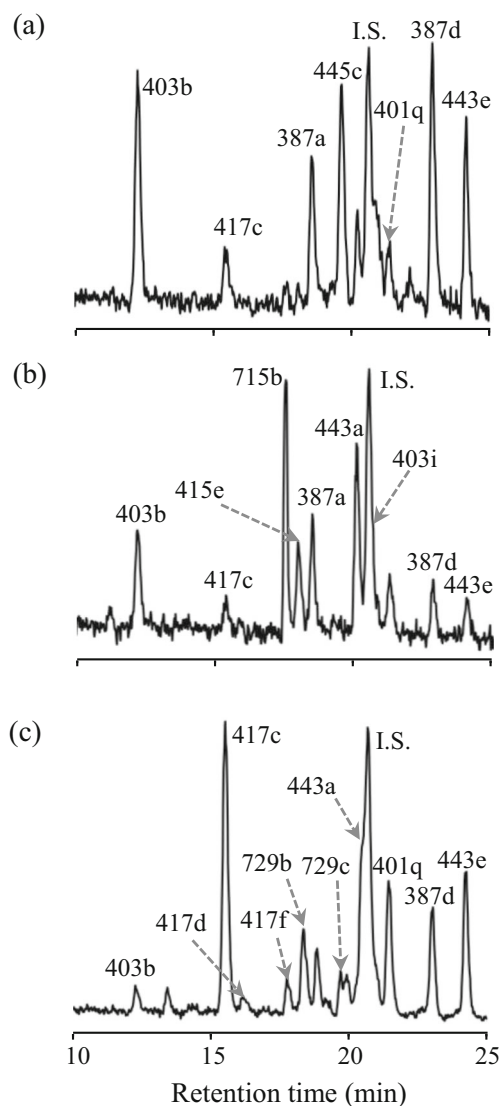
Fig. 2 Sample LCMS chromatograms of extracts from the three study taxa. (a) *B. j. japonicus* (b) *B. j. formosus* (c) *B. torrenticola*. Total ion chromatogram (TIC) is shown with tentative names of BDs. I.S.: internal standard, digitoxigenin

profiles of *B. j. japonicus* and *B. j. formosus*, as well as a strong association between the profiles of *B. torrenticola* and those of *B. j. formosus*.

Intra-Taxon Diversity of BD Profiles in B. j. japonicus The detection rate of cinobufagin and bufotalin in *B. j. japonicus* was significantly lower than in the other two taxa (Table 1). Furthermore, the rates of occurrence of 23 BDs in *B. j. japonicus* was significantly different between the C4 and C5 clusters (Supplemental Table S2). Of those 23 BDs, we identified two, bufotalin and bufotalin-3-suberoyl-L-arginine ester (B3sa) (Fig. 3b). Bufotalin was not detected in the Shikoku district, and B3sa was detected only in the Kyushu district (Supplemental Table S1). They were isolated by HPLC fractionation of parotoid gland secretion from *B. j. japonicus* and
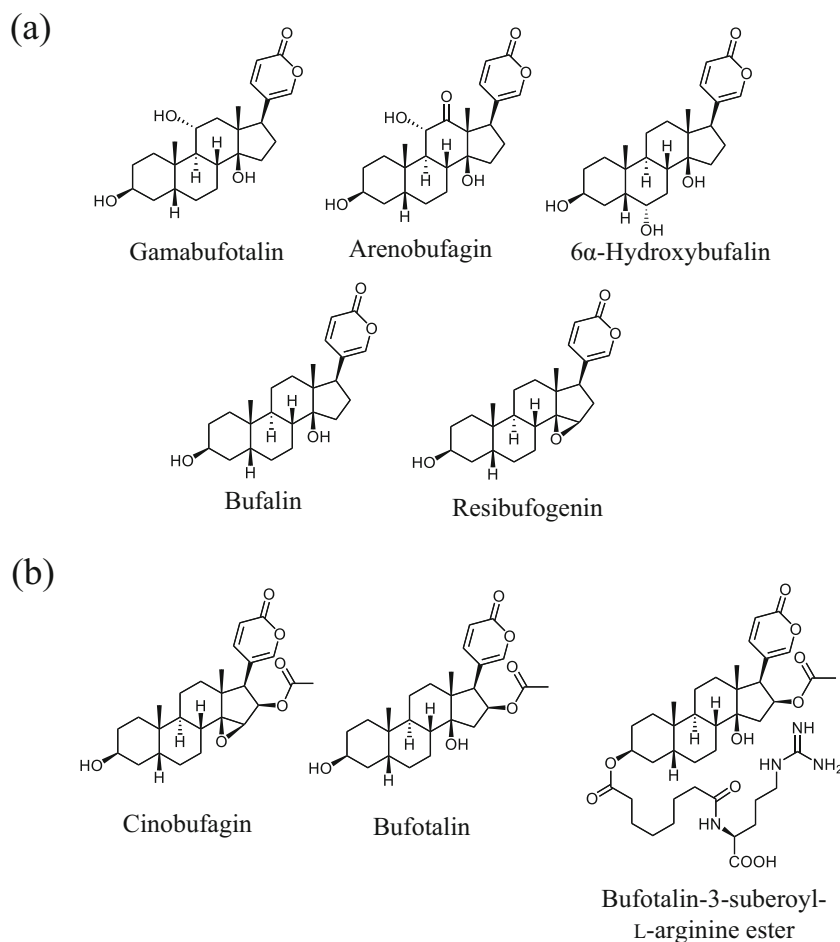
then identified by MS and various NMR analyses (see details in the following section).

Structure of BDs Eight BDs were isolated for structural analysis: gamabufotalin (7.6 mg), arenobufagin (2.0 mg), 6α-hydroxybufalin (3.2 mg), bufalin (2.5 mg), resibufogenin (1.6 mg), cinobufagin (2.6 mg), bufotalin (4.1 mg), and B3sa (4.0 mg). The structures of these compounds, except 6α-hydroxybufalin and B3sa, were assigned by employing ^{13}C NMR spectroscopy. The observed chemical shifts accorded with those of authenticated standards and literature values (Supplemental Table S3). Each molecular formula was predicted by high resolution LC/MS analyses, followed by LC/MS/MS analyses to indicate specific structures (Supplemental Table S4).

The structure of 6α-hydroxybufalin was determined by MS spectroscopy and NMR analyses. MS analysis showed the molecular formula as $C_{24}H_{34}O_5$ (Supplemental Table S4). In the ^{1}H-NMR spectrum, three signals derived from the pyrone ring [δ 8.00 (1H, dd), δ 7.43 (1H, d), δ 6.27 (1H, d)] and two signals derived from the methyl group [δ 1.10 (3H, s), δ 0.73 (3H, s)] were observed. Thus, this compound was presumed to be a BD with two methyl groups. From the spectral data of ^{1}H-NMR, ^{13}C-NMR, HSQC, and HMBC, four signals [δ 3.71 (1H, s, broad), δ 4.02 (1H, d), δ 1.10 (3H, s), and δ 0.73 (3H, s)] were assigned to 3-H$_α$, 6-H$_α$, 19-CH$_3$, and 18-CH$_3$, respectively. The relative stereochemistry was determined by NOESY (Supplemental Fig. S2A) as follows: The hydroxy group at position 6 was in the α position because 6-H correlated with 5-H$_β$, 7-H$_β$, and 8-H. The hydroxy group at position 3 was in the β position because 3-H correlated with 4-H$_α$, $_β$. The correlation between 19-CH$_3$ and 5-H indicated that the A/B ring fusion was *cis*. The correlation between 15-H and 7-H and correlation of 19-CH$_3$ with 8-H, 11-H, and 12-H showed that the B/C ring fusion was *trans* and the C/D fusion was *cis*. The pyrone rings of *Bufo*-derived BDs identified to date are all in the β position (Shimada et al. 1977; Steyn and van Heerden 1998; Wei et al. 2019); thus, the pyrone ring of this compound was also likely to be at the 17β position. The BD 6α-hydroxybufalin is a novel compound. The NMR data for this compound are summarized in supplemental Table S5.

The structure of B3sa also was determined by MS spectroscopy and NMR analyses (Supplemental Table S4 and S6, Supplemental Fig. S3). MS analysis showed the molecular formula as $C_{40}H_{60}N_4O_{10}$ (Supplemental Table S4). In the ^{1}H-NMR spectrum, three signals derived from the pyrone ring [δ 8.25 (1H, dd), δ 7.43 (1H, d), δ 6.20 (1H, d)] and two signals derived from the methyl group [δ 0.98 (3H, s), δ 0.78 (3H, s)] were observed. Thus, this compound was presumed to be a BD with two methyl groups. From the spectral data of ^{1}H-NMR, ^{13}C-NMR, HSQC, and HMBC, three signals [δ 5.08 (1H, s, broad), δ 1.10 (3H, s), and δ 0.73 (3H, s)] were assigned to 3-H$_α$, 19-CH$_3$, and 18-CH$_3$, respectively;

Fig. 3 Chemical structures of BDs identified in this study. (a) BDs occurring widely among the study taxa. (b) Cinobufagin: a component that exhibits large differences in detection rates between taxa; Bufotalin and B3sa: components with regional differences in the number of individuals in which these were detected

(a)

Gamabufotalin   Arenobufagin   6α-Hydroxybufalin

Bufalin   Resibufogenin

(b)

Cinobufagin   Bufotalin

Bufotalin-3-suberoyl-L-arginine ester

two signals of a carbonyl carbon (δ 172.1) and a methyl proton [δ 1.80 (3H, s)] were assigned the acetyl group at position 16. The relative stereochemistry was determined by NOESY (Supplemental Fig. S2B) as follows: The hydroxy group at position 3 was in the β position because 3-H correlated with 4-H$_{\alpha, \beta}$. The correlation between 19-CH$_3$ and 5-H indicated that the A/B ring fusion was *cis*. The correlation of 19-CH$_3$ with 8-H and 11-H and the correlation between 15-H and 7-H showed that the B/C ring fusion was *trans*, and the C/D fusion was *cis*. The stereochemistry of the pyrone ring was estimated as the β position as is the case for 6α-hydroxybufalin. Then, the acylation at position 3 was confirmed due to the downfield shift of 3-H [δ 5.08 (1H, s, broad)] compared with other BDs and HMBC correlation between 3-H and 1′ carbonyl carbon. This acyl group was presumed to be a saturated *n*-dicarboxylate conjugated with arginine. This arginine moiety was supported by imino carbon (δ 158.8), geminal coupling of 11′-H (δ 1.71 and δ 1.89), and HMBC correlation between 8′-C and 9′-H. Then, *n*-dicarboxylate moiety was determined by GC/MS analysis of B3sa hydrolysate. The methyl ether of liberated dicarboxylate accorded with dimethyl suberate (Supplemental Fig. S3). Therefore, the acyl group at position 3 was identified as suberoyl arginine. The absolute configuration of arginine was assumed as L because all known BDs with dicarboxyl arginine from *Bufo* possess L-arginine (Shimada et al. 1984, 1987; Steyn and van Heerden 1998). The NMR data for this compound are summarized in supplemental Table S6.

Discussion

Our LC/MS and NMR analyses demonstrate that all *Bufo* from mainland Japan possess BDs, including both widespread and uncommon compounds. Our HCA using the BD profiles obtained by LC/MS revealed that individuals of *B. j. formosus* are divided among clusters C1 and C3, excluding 6 individuals; individuals of *B. torrenticola* are placed in cluster C2, excluding 7 individuals; and individuals of *B. j. japonicus* are divided among clusters C4 and C5, excluding 4 individuals. These exceptions may reflect the occurrence of natural hybridization (Matsui and Maeda 2018; Yamazaki et al. 2008), the presence of introduced individuals outside of their native range (Hase et al. 2012), independent evolutionary origins of certain BD modifications, and/or misidentification of individual specimens.
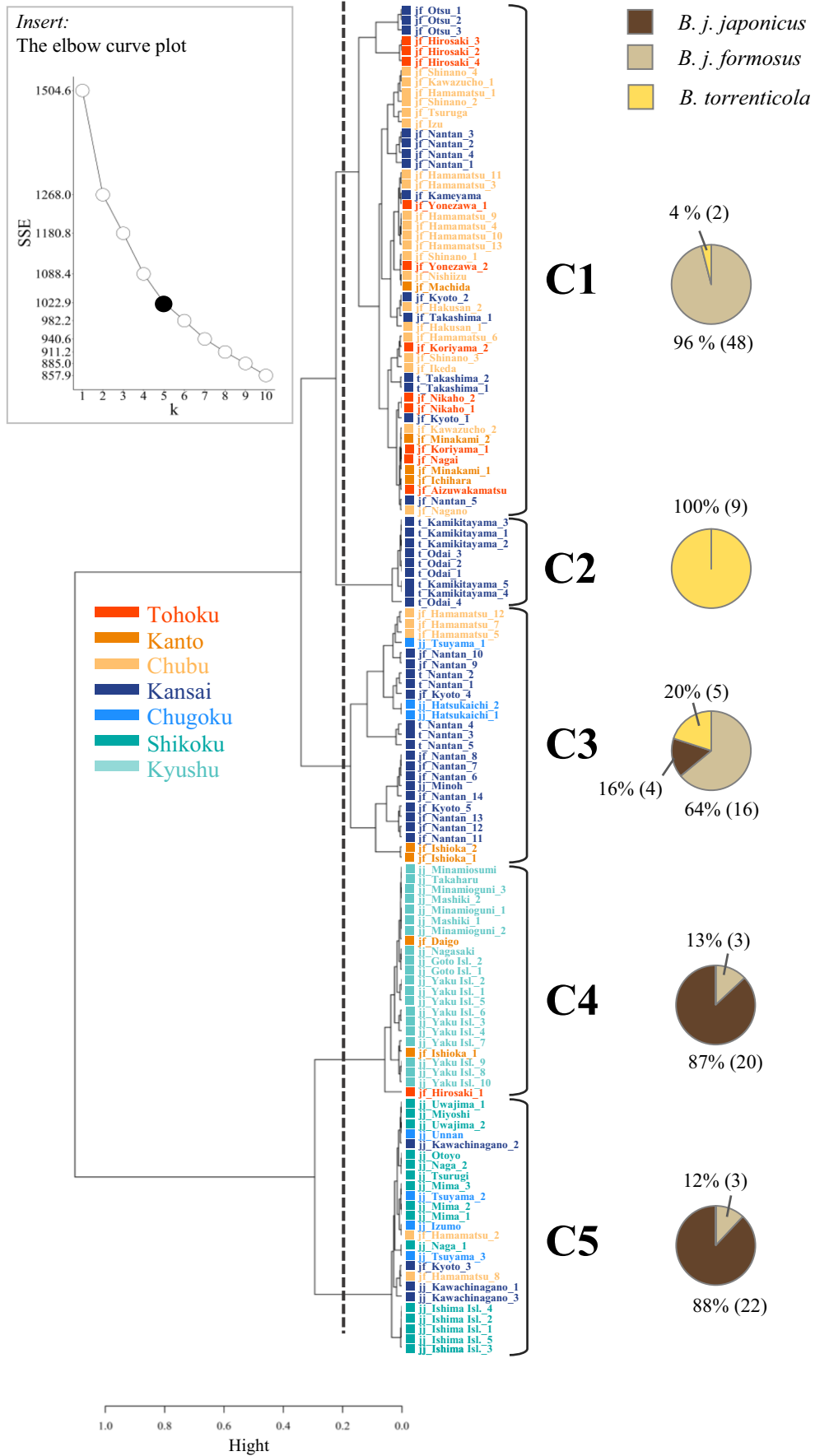
Fig. 4 The dendrogram generated by HCA based on BD profiles of individual toads. *Insert*: elbow curve plot with the number of primary clusters shown by a filled circle (k = 5). The broken line on the dendrogram reflects the number of primary clusters identified by the elbow method

The clustering indicates that BD profiles differ even within taxa, although it is unclear whether this diversity has been driven by adaptive or non-adaptive evolution. The clustering pattern we found largely reflects the geographical relationships among the clusters (Fig. 5). The border between the area of cluster C1, which covers the northern and eastern regions of the main island (the Tohoku, Kanto, and Chubu regions), and the adjoining clusters C2 and C3 (in the neighboring Kansai region) is presumed to be caused by expansion of an ancient basin in the Early Pliocene (ca. 5.7 Mya) (Igawa et al. 2006). The major area of cluster C4, Kyushu, is separated from the region of the adjoining cluster C5, Chugoku and Shikoku, by the sea. In the schematic map of Fig. 5, the roughly delineated areas of clusters C5 and C3 are depicted as geographically separated, but in fact these clusters include several localities in both the Kansai and Chugoku districts. Because the sampling in Kansai is biased toward a few particular sites and because the number of sampling localities in Chugoku is small, the geographic border between clusters C5 and C3 is, at present, unclear. Examination of BD profiles from more localities in the Kansai and Chugoku districts is necessary to clarify their geographic relationship. On the other hand, the independent clustering of C2, for which the geographic distribution is completely overlapped by that of C3, can be explained by the difference in their breeding habits: all individuals in C2 are *B. torrenticola*, which breeds in lotic water such

as mountain streams, whereas C3 mainly consists of *B. j. formosus*, which generally breeds in lentic water such as small temporary pools (Matsui and Maeda 2018).

Comparing the clustering pattern of BD profiles and the pattern for nucleotide sequences of the mitochondrial cytochrome *b* gene (Igawa et al. 2006), the two patterns are basically similar. The diversity of cytochrome *b* sequences is considered to result from the accumulation of neutral mutations, and therefore presumably results from a non-adaptive process, as in many other vertebrates (Irwin et al. 1991; Martin and Palumbi 1993). This suggests that the inter- and intra-specific diversity of BD profiles may also be driven by non-adaptive evolution, through neutral mutations in the BD metabolic pathway. However, the relationship of *B. torrenticola* relative to the other two taxa based on the BD profiles is different from that estimated by cytochrome *b* sequences. The BD profiles of cluster C2, which consists of *B. torrenticola* only, are similar to those of C1, which includes mainly *B. j. formosus* from eastern Japan, whereas Igawa et al. (2006) found a close evolutionary relationship between *B. torrenticola* and *B. j. japonicus* from western Japan. Therefore, the BD profiles do not seem to conform to the evolutionary history of *B. torrenticola*. This closer chemical similarity of *B. torrenticola* to *B. j. formosus* than to *B. j. japonicus* is partly due to the lower incidence of bufotalin and cinobufagin in *B. j. japonicus* than in the other two taxa (Table 1). We presume that this difference is caused by the loss of some metabolic capacities in *B. j. japonicus* (see below).

Our data on BD profiles provide insights into the metabolic system of BD synthesis in Japanese toads. The most consistently present compound is bufalin, which was detected in every individual of all three taxa, from all collecting sites.

Fig. 5 Schematic map of the geographical distribution of the five clusters, C1–5. Gray ellipses show the approximate distribution area of each cluster

Tohoku
Kanto
Chubu
Kansai
Chugoku
Shikoku
Kyushu
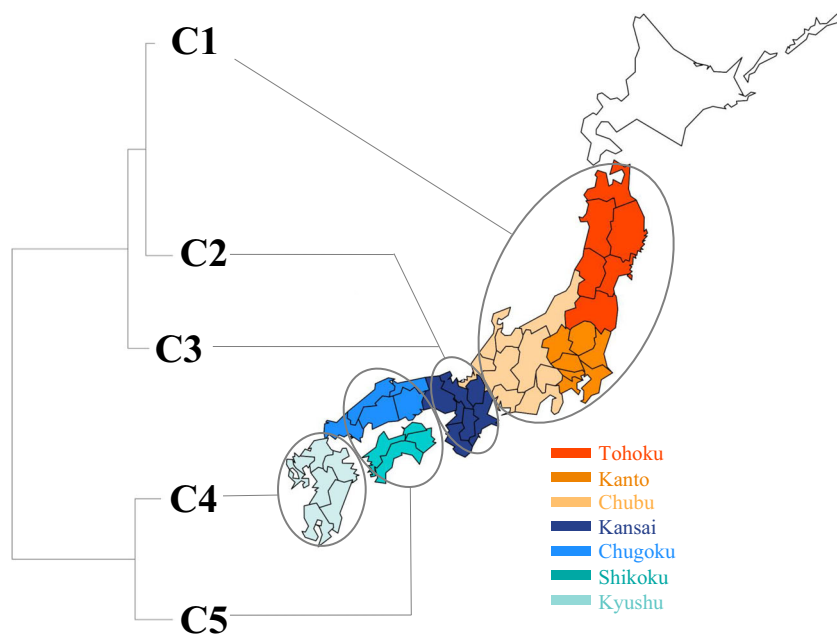
This suggests that bufalin may be located upstream in the BD biosynthetic pathway, as suggested by previous studies (Chen and Osuch 1969; and Porto et al. 1972). All other BDs we detected may be biosynthesized from bufalin by various modifications (Fig. 6). Here, we focus on the biosynthesis of bufotalin and cinobufagin, which could be produced by acetoxylation at 16-C of each corresponding precursor (steps 1 and 7 in Fig. 6). Their detection rate was lower in *B. j. japonicus* than in *B. torrenticola* and *B. j. formosus* (Table 1), suggesting that the metabolic capacity for acetoxylation may have been lost in some lineages of *B. j. japonicus*. Similar evolutionary changes within *B. j. japonicus* may be reflected in the regional differences we observed in the presence of specific BDs (Supplemental Table S2). On the other hand, the low rate of occurrence of B3sa suggests that the esterification ability for 3-OH (step 2 in Fig. 6) may have appeared among only a few lineages of *B. j. japonicus* and *B. j. formosus*. Indeed, many BDs occurred at low rates in this study (Table 1). These results suggest that the metabolic pathways underlying the modification of BDs in Japanese toads may be quite labile, resulting in the frequent loss or acquisition of specific compounds among local populations.

The hypothesis that the diversity of BDs in Japanese toads results from non-adaptive evolution associated with neutral mutations also is consistent with the existence of relatively few predators on those species. In some cases, biotoxins in animals coevolve as a consequence of an arms race between predators and prey (König et al. 2015; Roelants et al. 2010), although in some well-studied cases that involves increases in the quantity of toxins, rather than their diversity (Brodie III and Brodie Jr 1999; Hanifin 2010; Williams et al. 2003). In the case of *Bufo* in mainland Japan, there are few natural enemies except for *Rhabdophis tigrinus* (Hutchinson et al. 2007), and even that predator does not feed exclusively on toads. Furthermore, although BDs such as B3sa, with the suberoyl arginine chain at C-3 (known as bufotoxins), have been shown to be less toxic than compounds without that side chain, various BDs, including some of those identified in this study, have been tested and found to exhibit little difference in toxicity (Córdova et al. 2016; Kamano et al. 1998; Kamano et al. 2002; Tian et al. 2014). Therefore, though there are some exceptions, structurally different BDs may provide approximately equivalent protection against predators. Cluster C4, with a high detection rate of B3sa, which is expected to be
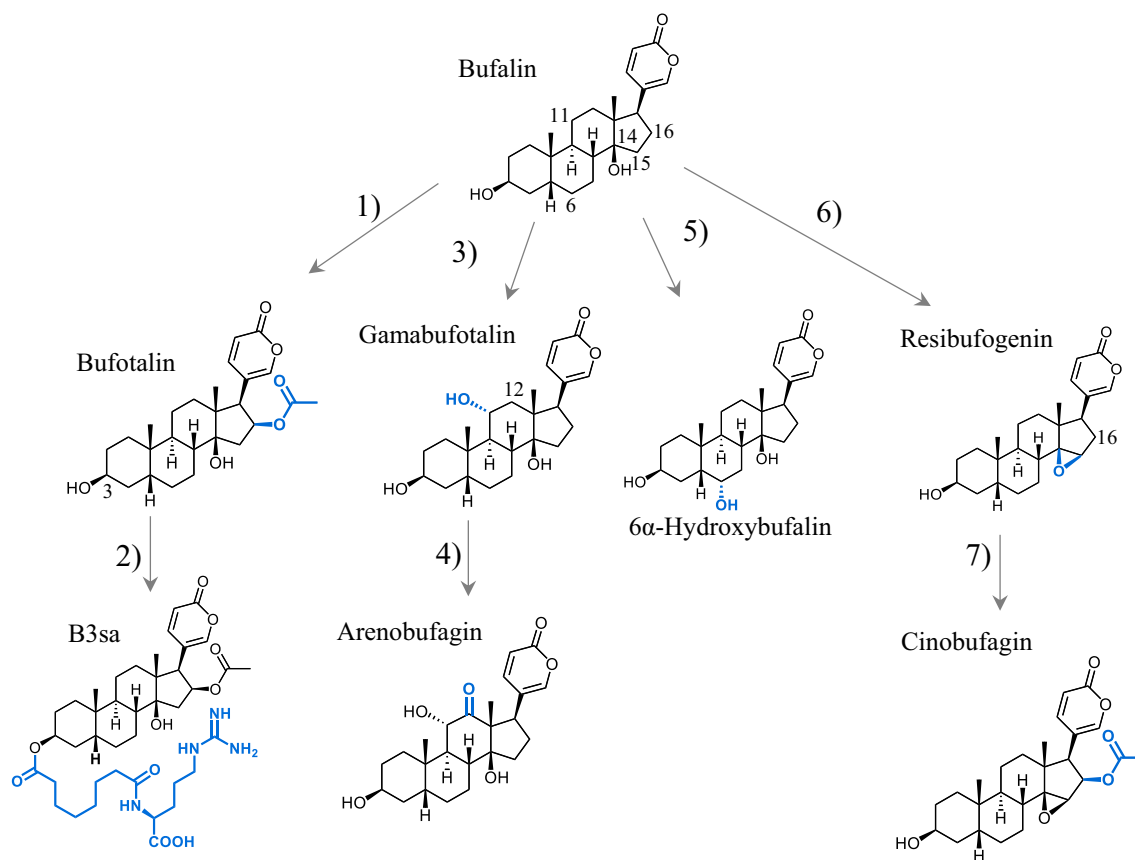

Fig. 6 The hypothesized chemical reactions from bufalin to the other BDs. The moiety formed in each reaction step is shown in blue. 1) Acetoxylation at 16-C of bufalin produces bufotalin; 2) esterification at 3-OH of bufotalin produces B3sa; 3) hydroxylation at 11-C of bufalin produces gamabufotalin; 4) oxidation at 12-C of gamabufotalin produces arenobufagin; 5) hydroxylation at C-6 of bufalin produces 6α-hydroxybufalin; 6) epoxidation at 14-C and 15-C of bufalin produces resibufogenin; 7) acetoxylation at 16-C of resibufogenin produces cinobufagin

less toxic to predators compared to other BDs, further suggests that diversification of BDs could be due to non-adaptive evolution.

Diversity of BDs in Japanese toads is high (Supplemental Table S1) in spite of the presumably weak selective pressure. The shared moieties among BDs in toads, including C/D *cis*-conformation and the pyrone ring at position 17, which are fundamental and conserved aspects of the molecular structures, apparently serve to impart strong toxicity to BDs (Kamano et al. 1998; Liu et al. 2018; Steyn and van Heerden 1998). The further diversification of BDs may subsequently have been driven by rapid mutations in the enzymes that further modify this basic bufadienolide structure (e.g*.,* hydroxylation, acetoxylation, and esterification). Indeed, Shibata et al. (2018) suggested the presence of molecular mechanisms to rapidly diversify venom genes in the Japanese habu (*Protobothrops flavoviridis*), a viperid snake. Our analysis of BD profiles from Japanese toads appears to demonstrate that toxin diversity can occur under weak selection pressure related to environmental variables, rather than under strong selection pressures, as in arms races. The model seen in the Japanese toads may also apply to the diversity of defensive toxins in various other animals.

Data Availability Uploading and archiving of auxiliary data files is not required as all data related to this manuscript is contained in the supplementary material.

Compliance with Ethical Standards

Conflict of Interest Not applicable.

Ethics Approval The present study was carried out in compliance with the guidelines of the Animal Care and Use Committee of Kyoto University.

Consent to Participate Not applicable.

Consent for Publication We consent to publication.

Code Availability Not applicable

References

Barbosa CM, Medeiros MS, Riani Costa CCM, Camplesi AC, Sakate M (2009) Toad poisoning in three dogs: case reports. J Venom Anim Toxins 15:789–798. https://doi.org/10.1590/S1678-91992009000400016

Brodie ED III, Brodie ED Jr (1999) Predator-prey arms races: asymmetrical selection on predators and prey may be reduced when prey are dangerous. BioScience 49:557–568. https://doi.org/10.2307/1313476

Casewell NR, Wüster W, Vonk FJ, Harrison RA, Fry BG (2013) Complex cocktails: the evolutionary novelty of venoms. Trends Ecol Evol 28:219–229. https://doi.org/10.1016/j.tree.2012.10.020

Chen C, Osuch MV (1969) Biosynthesis of bufadienolides–3β-hydroxycholanates as precursors in *Bufo marinus* bufadienolides synthesis. Biochem Pharmacol 18:1797–1802. https://doi.org/10.1016/0006-2952(69)90273-1

Córdova WHP, Leitao SG, Cunha-Filho G, Bosch RA, Alonso IP, Pereda-Miranda R, Gervou R, Touza NA, Quintas LEM, Noel F (2016) Bufadienolides from parotoid gland secretions of Cuban toad *Peltophryne fustiger* (Bufonidae): inhibition of human kidney Na$^+$/K$^+$-ATPase activity. Toxicon 110:27–34. https://doi.org/10.1016/j.toxicon.2015.11.015

Dumbacher JP, Wako A, Derrickson SR, Samuelson A, Spande TF, Daly JW (2004) Melyrid beetles (*Choresine*): a putative source for the batrachotoxin alkaloids found in poison-dart frogs and toxic passerine birds. Proc Natl Acad Sci U S A 101:15857–15860. https://doi.org/10.1073/pnas.0407197101

Green B, Crane RI, Khaidem IS, Leighton RS, Newaz SS, Smyser TE (1985) Synthesis of steroidal 16, 17-fused unsaturated–lactones. J Org Chem 50:640–644. https://doi.org/10.1021/jo00205a016

Hanifin CT (2010) The chemical and evolutionary ecology of tetrodotoxin (TTX) toxicity in terrestrial vertebrates. Mar Drugs 8:577–593. https://doi.org/10.3390/md8030577

Hase K, Shimada M, Nikoh N (2012) High degree of mitochondrial haplotype diversity in the Japanese common toad *Bufo japonicus* in urban Tokyo. Zool Sci 29:702–708. https://doi.org/10.2108/zsj.29.702

Hashimoto N, Aoyama T, Shiori T (1981) A simple efficient preparation of methyl esters with trimethylsilyldiazomethane (TMSCHN) and its application to gas chromatographic analysis of fatty acids. Chem Pharm Bull 29:1475–1478. https://doi.org/10.1248/cpb.29.1475

Hirai T, Matsui M (2002) Feeding ecology of Bufo japonicus formosus from the montane region of Kyoto, Japan. J Herpetol 36:719–723.

https://doi.org/10.1670/0022-1511(2002)036[0719:FEOBJF]2.0.CO;2

Hostetler JR, Cannon MS (1974) The anatomy of the parotoid gland in Bufonidae with some histochemical findings. J Morphol 142:225–239. https://doi.org/10.1002/jmor.1051420208

Hutchinson DA, Mori A, Savitzky AH, Burghardt GM, Wu X, Meinwald J, Schroeder FC (2007) Dietary sequestration of defensive steroids in nuchal glands of the Asian snake *Rhabdophis tigrinus*. Proc Natl Acad Sci U S A 104:2265–2270. https://doi.org/10.1073/pnas.0610785104

Hutchinson DA, Savitzky AH (2004) Vasculature of the parotoid glands of four species of toads (Bufonidae: *Bufo*). J Morphol 260:247–254. https://doi.org/10.1002/jmor.10219

Igawa T, Kurabayashi A, Nishioka M, Sumida M (2006) Molecular phylogenetic relationship of toads distributed in the Far East and Europe inferred from the nucleotide sequences of mitochondrial DNA genes. Mol Phylogenet Evol 38:250–260. https://doi.org/10.1016/j.ympev.2005.09.003

Irwin DM, Kocher TD, Wilson AC (1991) Evolution of the cytochrome *b* gene of mammals. J Mol Evol 32:128–144. https://doi.org/10.1007/BF02515385

Kamano Y, Kotake A, Hashima H, Inoue M, Morita H, Takeya K, Itokawa H, Nandachi N, Segawa T, Yukita A, Saitou K, Katsuyama M, Pettit GR (1998) Structure-cytotoxic activity relationship for the toad poison bufadienolides. Bioorg Med Chem 6:1103–1115. https://doi.org/10.1016/S0968-0896(98)00067-4

Kamano Y, Yamashita A, Nogawa T, Morita H, Takeya K, Itokawa H, Segawa T, Yukita A, Saito K, Katsuyama M, Pettit GR (2002) QSAR evaluation of the Ch'an Su and related bufadienolides against the colchicine-resistant primary liver carcinoma cell line PLC/PRF/51. J Med Chem 45:5440–5447. https://doi.org/10.1021/jm0202066

Kodinariya TM, Makwana PR (2013) Review on determining number of cluster in k-means clustering. IJCSMS 1:90–95 ISSN: 2321–7782

König E, Bininda-Emondsa ORP, Shaw C (2015) The diversity and evolution of anuran skin peptides. Peptides 63:96–117. https://doi.org/10.1016/j.peptides.2014.11.003

Licht LE, Low B (1968) Cardiac response of snakes after ingestion of toad parotoid venom. Copeia 1968:547–551. https://www.jstor.org/stable/1442023

Lichtstein D, Samuelov S, Gati I, Wechter WJ (1992) Digitalis-like compounds in animal tissues. J Basic Clin Physiol Pharmacol 3:269–292. https://doi.org/10.1515/JBCPP.1992.3.4.269

Liu H, Chen SY, Guo JY, Su P, Qiu YK, Ke CH, Feng DQ (2018) Effective natural antifouling compounds from the plant *Nerium oleander* and testing. Int Biodeterior Biodegradation 127:170–177. https://doi.org/10.1016/j.ibiod.2017.11.022

Martin AP, Palumbi SR (1993) Protein evolution in different cellular environments: cytochrome *b* in sharks and mammals. Mol Biol Evol 10:873–891. https://doi.org/10.1093/oxfordjournals.molbev.a040047

Marutho D, Handaka SH, Wijaya E, Muljono (2018) The determination of cluster number at k-mean using elbow method and purity evaluation on headline news (2018) 2018 Int'l Seminar on App for Tech of Info and Comm, Semarang: 533–538. https://ieeexplore.ieee.org/stamp/stamp.jsp?tp=&arnumber=8549751

Matsui M (1984) Morphometric variation analyses and revision of the Japanese toads (genus Bufo, Bufonidae). Contr Biol Lab Kyoto Univ 26:209–428. http://hdl.handle.net/2433/156031

Matsui M, Maeda N (2018) Encyclopaedia of Japanese frogs. Bun-ichi Sogo Shuppan, Tokyo

Mebs D (2001) Toxicity in animals. Trends in evolution? Toxicon 39:87–96. https://doi.org/10.1016/S0041-0101(00)00155-0

Mohammadi S, Petschenka G, French SS, Mori A, Savitzky AH (2018) Snakes exhibit tissue-specific variation in cardiotonic steroid sensitivity of Na^+/K^+-ATPase. Comp Biochem Physiol B 217:21–26. https://doi.org/10.1016/j.cbpb.2017.11.014

Mori A, Burghardt GM, Savitzky AH, Roberts KA, Hutchinson DA, Goris RC (2012) Nuchal glands: a novel defensive system in snakes. Chemoecology 22:187–198. https://doi.org/10.1007/s00049-011-0086-2

Porto AM, Baralle FE, Gros EG (1972) Biosynthesis of bufadienolides in toads: III–experiments with [2-^{14}C] mevalonic acid, [20-^{14}C] 3β-hydroxy-5-pregnen-20-one and [20-^{14}C] cholesterol. J Steroid Biochem 3:11–17. https://doi.org/10.1016/0022-4731(72)90006-4

Roelants K, Fry BG, Norman JA, Clynen E, Schoofs L, Bossuyt F (2010) Identical skin toxins by convergent molecular adaptation in frogs. Curr Biol 20:125–130. https://doi.org/10.1016/j.cub.2009.11.015

Shibata H, Chijiwa T, Oda-Ueda N, Nakamura H, Yamaguchi K, Hattori S, Matsubara K, Matsuda Y, Yamashita A, Isomoto A, Mori K, Tashiro K, Kuhara S, Yamasaki S, Fujie M, Goto H, Koyanagi R, Takeuchi T, Fukumaki Y, Ohno M, Shoguchi E, Hisata K, Satoh N, Ogawa T (2018) The habu genome reveals accelerated evolution of venom protein genes. Sci Rep 8:11300 https://www.nature.com/articles/s41598-018-28749-4.pdf

Shimada K, Fujii Y, Mitsuishi E, Nambara T (1974) Isolation of a new type bufotoxin from skin of Bufo vulgaris formosus Boulenger. Tetrahedron Lett 15:467–468. https://doi.org/10.1016/S0040-4039(01)82245-0

Shimada K, Sato Y, Fujii Y, Nambara T (1976) Occurrence of bufalitoxin, cinobufotoxin and their homologs in Japanese toad. Chem Pharm Bull 24:1118–1120. https://doi.org/10.1248/cpb.24.1118

Shimada K, Fujii Y, Yamashita E, Niizaki Y, Sato Y, Nambara T (1977) Studies on cardiotonic steroids from the skin of Japanese toad. Chem Pharm Bull 25:714–730. https://doi.org/10.1248/cpb.25.714

Shimada K, Ohishi K, Nambara T (1984) Isolation and characterization of new bufotoxins from the skin of Bufo melanostictus Schneider. Chem Pharm Bull 32(11):4396–4401

Shimada K, Ro JS, Kanno C, Nambara T (1987) Occurrence of bufogenin conjugates in the skin of Korean toad. Chem Pharm Bull 35(12):4996–4999

Steyn PS, van Heerden FR (1998) Bufadienolides of plant and animal origin. Nat Prod Rep 15:397–413. https://pubs.rsc.org/en/content/articlepdf/1998/np/a815397y

Syakur MA, Khotimah BK, Rochman EMS, Satoto BD (2018) Integration k-means clustering method and elbow method for identification of the best customer profile cluster. Iop Conf Ser Mater Sci Eng 336:012017. https://iopscience.iop.org/article/10.1088/1757-899X/336/1/012017/pdf

Takada W, Sakata T, Shimano S, Enami Y, Mori N (2005) Scheloribatid mites as the source of pumiliotoxins in dendrobatid frogs. J Chem Ecol 31:2403–2415. https://doi.org/10.1007/s10886-005-7109-9

Tian HY, Zhang PW, Liu JS, Zhang DM, Zhang XQ, Jiang RW, Ye WC (2014) New cytotoxic C-3 dehydrated bufadienolides from the venom of *Bufo bufo gargarizans*. Chin Chem Lett 25:1104–1106. https://doi.org/10.1016/j.cclet.2014.02.006

Toledo RC and Jared C (1995) Cutaneous granular glands and amphibian venoms. Comp Biochem Phys A 111: 1–29. https://doi.org/10.1016/0300-9629(95)98515-I

Wei WL, Hou JJ, Wang X, Yu Y, Li HJ, Li ZW, Feng ZJ, Qu H, Wu WY, Guo DA (2019) *Venenum bufonis*: an overview of its traditional use, natural product chemistry, pharmacology, pharmacokinetics and toxicology. J Ethnopharmacol 237:215–235. https://doi.org/10.1016/j.jep.2019.03.042

Williams BL, Brodie ED Jr, Brodie ED III (2003) Coevolution of deadly toxins and predator resistance: self-assessment of resistance by garter snakes leads to behavioral rejection of toxic newt prey. Herpetologica 59:155–163. https://doi.org/10.1655/0018-0831(2003)059[0155:CODTAP]2.0.CO;2

Williams BL, Brodie ED Jr, Brodie ED III (2004) A resistant predator and its toxic prey: persistence of newt toxin leads to poisonous (not venomous) snakes. J Chem Ecol 30:1901–1919. https://doi.org/10.1023/B:JOEC.0000045585.77875.09

Yamazaki Y, Kouketsu S, Fukuda T, Araki Y, Nambu H (2008) Natural hybridization and directional introgression of two species of

Japanese toads *Bufo japonicus formosus* and *Bufo torrenticola* (Anura: Bufonidae) resulting from changes in their spawning habitat. J Herpetol 42:427–436. https://doi.org/10.1670/07-186.1

Yang Q, Zhou X, Zhang M, Bi L, Miao S, Cao W, Xie Y, Sun J, Tang H, Li Y, Miao Q, Wang S (2015) Angel of human health: current research updates in toad medicine. Am J Transl Res 7: 1–14. https://www.ncbi.nlm.nih.gov/pmc/articles/PMC4346519/pdf/ajtr0007-0001.pdf

Yoshida T, Ujiie R, Savitzky AH, Jono T, Inoue T, Yoshinaga N, Aburaya S, Aoki W, Takeuchi H, Ding L, Chen Q, Cao C, Tsai TS, de Silva A, Mahaulpatha D, Nguyen TT, Tang Y, Mori N, Mori A (2020) Dramatic dietary shift maintains sequestered toxins in chemically defended snakes. Proc Natl Acad Sci U S A 117: 5964–5969. https://doi.org/10.1073/pnas.1919065117

Zhao HY, Wu FK, Qiu YK, Wu Z, Jiang YT, Chen JY (2010) Studies on cytotoxic constituents from the skin of the toad *Bufo bufo gargarizans*. J Asian Nat Prod Res 12:793–800. https://doi.org/10.1080/10286020.2010.505187